Journal of Non-Crystalline Solids 354 (2008) 4730–4736

Contents lists available at ScienceDirect

Journal of Non-Crystalline Solids

journal homepage: www.elsevier.com/locate/jnoncrysol

Effect of cooling on the optical properties and crystallization of UV-exposed photo-thermo-refractive glass

Julien Lumeau [a,*], Larissa Glebova [a], Guilherme P. Souza [b], Edgar D. Zanotto [b], Leonid B. Glebov [a]

[a] CREOL, University of Central Florida, 4000, Central Florida Blvd, Orlando, FL 32816-2700, USA
[b] Vitreous Materials Laboratory, LaMaV, Department of Materials Engineering, DEMa, Federal University of São Carlos, UFSCar 13565-905, São Carlos, SP, Brazil

ARTICLE INFO

Article history:
Available online 23 August 2008

PACS:
42.70.Ce
42.40.Eq
61.46.Hk
78.20.Ci
81.40.−z

Keywords:
Crystallization
Optical microscopy
Nanocrystals
Absorption
Lasers
Optical spectroscopy
Photoinduced effects
Calorimetry

ABSTRACT

Photo-thermo-refractive (PTR) glass is a multi-component silicate glass that undergoes a refractive index change after UV-exposure and thermal treatment. This photo-thermo-refractivity is due to the precipitation of sodium fluoride nano-crystals; thus the glass remains highly transparent in the visible and near-IR regions. Up to now, most studies focused on the influence of temperature and duration of thermal treatment on the PTR glass properties, but no attention was given to the cooling step after thermal treatment. In this paper, the influence of cooling on crystallization and resulting optical properties of UV-exposed PTR glass is studied. We show that cooling between the nucleation and growth treatments is a mandatory step to achieve the full benefits of the first heat-treatment, i.e., a large number of small crystals. We also show that the main part of the refractive index change occurs on the cooling path after pre-nucleation. Non-isothermal DSC study associated with in situ pre-nucleation treatment shows that pre-nucleation enhances crystallization only if the temperature is decreased below T_g before the second (development) treatment. Using high temperature photometric measurements of the absorption spectra of UV-exposed PTR glasses, we tentatively associate that effect with the presence of liquid drops of a silver containing phase during regular pre-nucleation treatment. This fact explains the necessity to cool such drops below their melting point to obtain nucleation centers for efficient precipitation of NaF nano-crystals.

1. Introduction

Photo-thermo-refractive (PTR) glass is a sodium–zinc–aluminum–silicate glass containing small amounts of fluorine and bromine, doped with cerium, silver, antimony, and tin. Glasses which undergo photo-thermo induced crystallization were invented many years ago by Stookey [1] and have been studied as possible candidates for hologram writing in the last 15 years [2–5]. PTR glass exhibits significant refractive index change after UV-exposure and thermal treatments (pre-nucleation + development) above the glass transition temperature, T_g, which results from the crystallization of about 0.1 wt% sodium fluoride nanocrystals [6]. After partial crystallization the glass remains highly transparent in the visible. Therefore, the possibility of recording phase holograms in this type of glass has numerous potential applications, such as optical filtering [7] or spectral beam combining [8]. A simplified description of the complex photo-thermo crystallization mechanisms is given in Ref. [9].

The evolution of the crystallization and optical properties of PTR glass after UV-exposure is reported in several publications [6,10–14], and described in reviews, e.g. [15]. In this paper, we first analyze the correlation between the end temperature before quenching and the refractive index change that occurs after the thermal development of a UV-exposed PTR glass sample. Then, we show the effect of cooling on the crystallization kinetics and microstructure of UV-exposed PTR glass. In a complementary analysis of crystallization, the effect of cooling temperature is studied by non-isothermal differential scanning calorimetry. Finally, the evolution of the nucleation process is followed by spectro-photometric measurements. Insights on the mechanism of nucleation in PTR glass are advanced.

2. Experimental – materials and methods

2.1. Glass sample preparation

Samples of a photosensitive PTR glass containing $15Na_2O$–$5ZnO$–$4Al_2O_3$–$70SiO_2$–$5NaF$–$1KBr$–$0.01Ag_2O$–$0.01CeO_2$ (mol%) and minor amounts of Sn and Sb were used in this work as in

* Corresponding author. Tel.: +1 321 948 5115.
E-mail address: jlumeau@creol.ucf.edu (J. Lumeau).

0022-3093/$ - see front matter © 2008 Elsevier B.V. All rights reserved.
doi:10.1016/j.jnoncrysol.2008.06.103

previous studies [3–6]. The glass was melted in an electric furnace in a 0.5 l platinum crucible at 1460 °C for 5 h in air. Stirring with a Pt blade was used to homogenize the liquid. After melting, homogenizing and fining, the glass was cooled to the glass transition temperature ($T_g \sim 460$ °C), then annealed at T_g for 2 h, and cooled to room temperature at a rate of 0.1 K/min. Polished $25 \times 25 \times 2$ mm^3 samples were prepared from the batch. The chemical homogeneity of the samples is a critical parameter affecting crystallization properties [16], thus homogeneity was tested by the shadow method in a divergent beam of a He–Ne laser and was quantified by measurements using an interferometer (GPI Zygo). The samples selected for this study had refractive index fluctuations of less than 40 ppm (peak-to-valley) across the aperture. UV-exposure of samples was performed by a He–Cd laser (4 mW, 325 nm). Except for the characterization of the refractive index change (Section 2.2), all samples were homogeneously exposed with a dosage of 0.9 J/cm^2.

2.2. Photosensitivity characterization

The method used for characterizing the photosensitivity of PTR glass was the same as in Ref. [10]. Glass samples for refractive index measurements were fixed onto a computer-controlled translation stage and moved across a laser beam (He–Cd laser, 4 mW, 325 nm) at constant velocity in order to record a stripe with controlled distribution of dosages (Gaussian distribution with maximum of 0.9 J/cm^2). After exposure, the samples were thermally developed for 30 min at 520 °C. Refractive index changes were measured in each sample using a shearing interferometer setup [10]. Its basic principle is to create an interferogram that converts the phase change at propagation through the glass to a fringe shift. A liquid cell with an index matching fluid was used to prevent thickness variations of the sample which would contribute to fringe shift. Therefore the interferometer fringe distortions resulted only from refractive index variations.

2.3. Differential scanning calorimeter (DSC) measurements

Thermal analysis was performed using a DSC (Q10 DSC, TA Instruments) with sample weights of typically 30 mg and a heating rate of 30 K/min. Pre-nucleation of the samples was carried out in situ, inside the heating chamber of the DSC. DSC curves are shown in the temperature range of 500–720 °C, where relevant thermal events take place. The position of the maximum of the exothermic peak was denominated crystallization temperature, T_c.

2.4. Absorption spectra measurements

Optical absorption spectra were measured with the setup shown in Fig. 1. It is composed of a UV/visible white light (deuterium tungsten halogen) source. Light is coupled inside a 200 μm fiber and then collimated using a lens. The beam diameter is around 2 mm. This beam passes through the sample and is collected by a collimator associated with a 200 μm fiber. The collected light is sent to an Ocean Optics S2000 spectrometer that allows for spectral measurement of the transmitted power in the range of 380 up to 800 nm. The sample is placed inside a heating cell, which guarantees precise control of temperature in the range of 25 up to 600 °C. Therefore, this cell was also used for the thermal treatments of the samples. The transmitted power (P_s) was measured in situ for different durations of thermal treatment. In order to convert these power measurements into absorption spectra, preliminary measurements were carried out. The power was first measured when the beam was hidden ($P_{0\%}(\lambda)$), then a new measurement was performed with no sample placed in the sample holder ($P_{100\%}(\lambda)$). Finally, absorption spectra ($A(\lambda)$) were calculated as follows:

$$A(\lambda) = -\frac{1}{t}\log(T(\lambda) - R(\lambda)) = -\frac{1}{t}\log\left(\frac{P_s(\lambda) - P_{0\%}(\lambda)}{P_{100\%}(\lambda) - P_{0\%}(\lambda)} - R(\lambda)\right), \quad (1)$$

where t is the sample thickness ($t \sim 1.2$ mm) and $R(\lambda)$ the losses corresponding to Fresnel reflections on the faces of PTR glass sample, previously determined.

3. Results

3.1. Effect of cooling temperature on refractive index change

Several homogeneous samples from the same melt were prepared with the method described in Section 2.1. Each sample was UV-exposed with a Gaussian stripe and dosage of 0.9 J/cm^2 at 325 nm, and then heat-treated for 30 min at 520 °C to induce partial crystallization, which triggered a refractive index change. In order to study the effect of cooling, samples were left inside the hot furnace where unforced decrease of temperature in furnace occurred (estimated rate of ~2.5 °C/min). Each sample was then quenched (drawn from the furnace and placed on top of a metal plate at room temperature) from a different temperature starting at 520 °C down to 420 °C with a 20 °C step. A typical thermal treatment schedule is shown in Fig. 2a. Refractive index was measured using the liquid-cell shearing interferometer. The refractive index change was also measured in a sample that was not quenched from high temperature, but annealed down to room temperature (left cooling down inside the furnace). Evolution of the ratio between refractive index changes measured in each quenched sample and

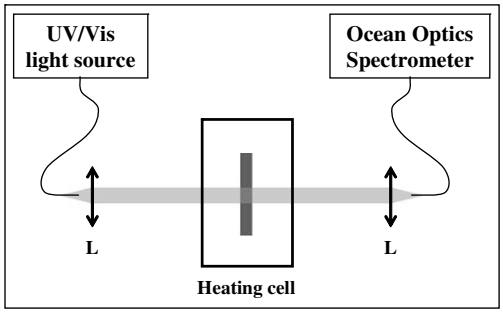

Fig. 1. Spectrometric setup developed for the measurement of the evolution, at high temperature, of the absorption band of silver containing particles in PTR glass.

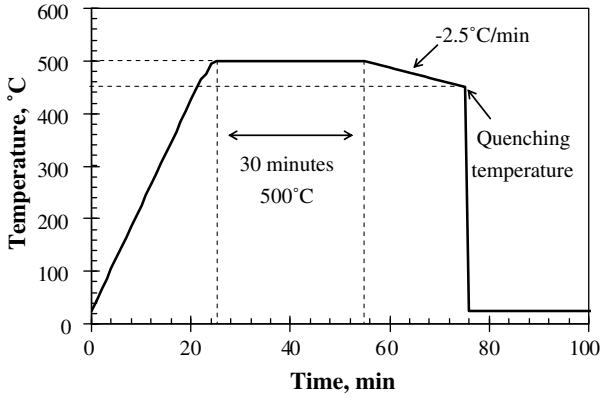

Fig. 2a. Thermal treatment schedule used for the analysis of the influence of cooling on PTR glass refractive index change.

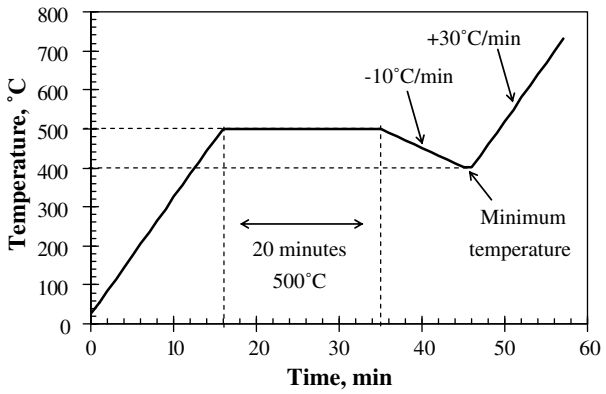

Fig. 2b. Thermal treatment schedule used for the analysis of the influence of cooling on DSC thermograms.

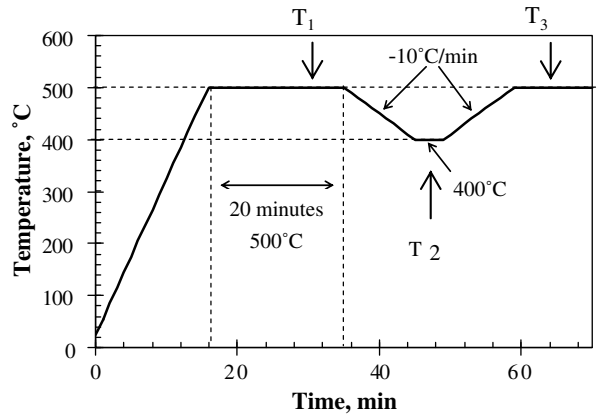

Fig. 2c. Thermal treatment schedule used for the analysis of the influence of cooling on the absorption band of silver containing particles.

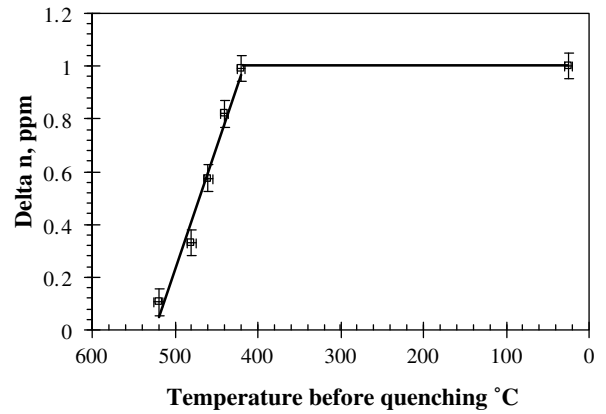

Fig. 3. Evolution of refractive index change during the cooling process as a function of quenching temperature.

of that of the annealed sample was plotted as a function of quenching temperature (Fig. 3). One can see that quenching from a temperature very close to that of the thermal development does not lead to large refractive index changes in UV-exposed PTR glass. As a result, the lower the quenching temperature, the higher the refractive index change. Refractive index change saturates at 420 °C.

3.2. Effect of cooling on microstructure and crystallization kinetics

The effect of cooling on the PTR glass microstructure was also studied. Two PTR glass samples were UV-exposed to 0.9 J/cm^2 at 325 nm. One sample was developed for 30 min at 650 °C, and the other underwent six successive thermal treatments of 5 min each. The temperature of thermal development (650 °C) was chosen to allow for crystal growth to micron-size. After each of these treatments, optical micrographs were recorded using a Leica DMRX optical microscope, coupled with a GKB (CC-8703) high-resolution CCD color camera and a 100× objective. Transmitted-light micrographs obtained after these thermal treatments are shown in Fig. 4. One can notice that samples heat-treated with successive steps have crystals with small diameter, <3 μm. A very fine structure can be observed in the glass matrix surrounding these crystals. On the other hand, the sample that underwent uninterrupted development for 30 min at 650 °C shows large crystals with dendritic shape, but no fine structure in the surrounding glass. Evolution of the crystal size as a function of thermal development duration, for each of the procedures (multi-step and uninterrupted), is shown in Fig. 5. In the multi-step heat-treatments, crystal size saturated after 5 min and showed no further increase. In contrast, if continuous heat-treatment is used, the crystals grow about 2.5 times larger, reaching a diameter of about 7 μm (size at saturation is limited by the NaF content in the original glass).

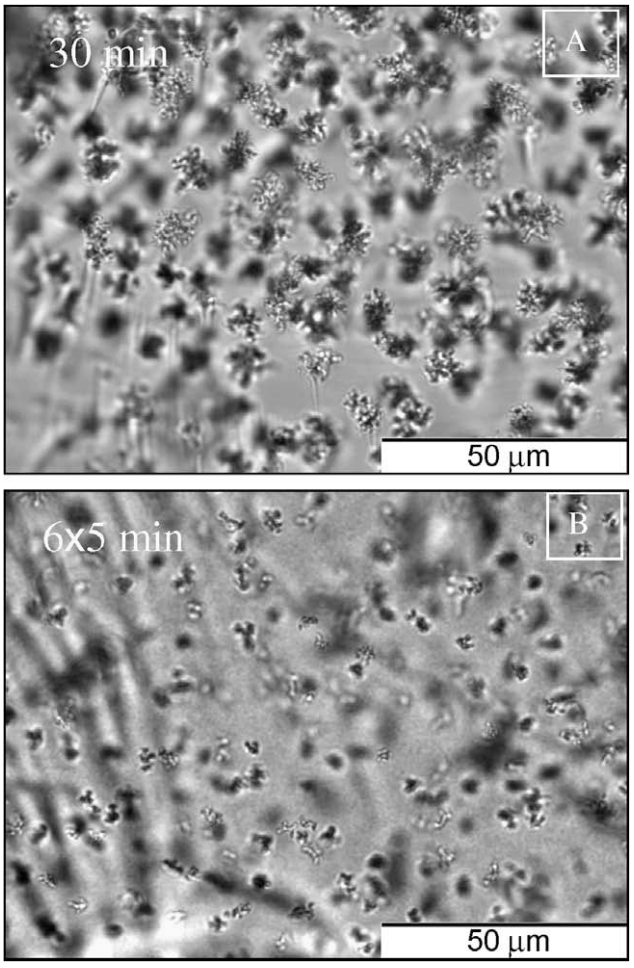

Fig. 4. Optical micrographs of UV-exposed PTR glass treated for 30 min at 650 °C – (A) continuous heat-treatment and (B) multi-step heat-treatment.

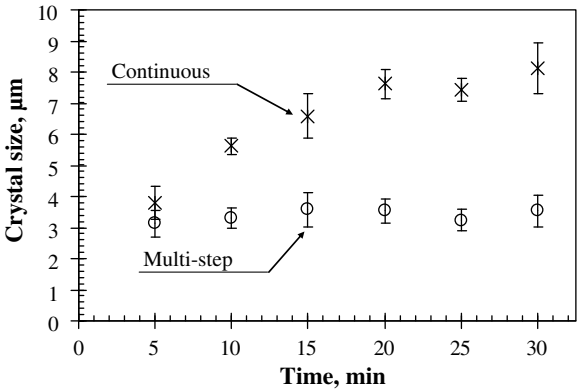

Fig. 5. Crystal growth curve of UV-exposed PTR glass as a function of treatment time at 650 °C – circles represent the maximum crystal size measured after 5-min multi-step heat-treatment and stars represents the maximum crystal size measured after continuous heat-treatment.

3.3. Effect of cooling on DSC traces

DSC was used to study the effect of cooling on the overall crystallization of UV-exposed PTR glass. All heat-treatments were carried out in situ, i.e. inside the DSC. A typical heat-treatment schedule is shown in Fig. 2b. The DSC was programmed to first increase the temperature up to 500 °C, then to stabilize at 500 °C to perform an isothermal nucleation step for 20 min (at 500 °C), followed by a decrease of temperature down to a given temperature (from 400 to 500 °C, i.e. no cooling to room temperature) with controlled cooling rate of 10 °C/min. Then, DSC traces were recorded starting from the lowest temperature reached up to 720 °C, and the resulting DSC traces were plotted in the range from 500 to 720 °C (Fig. 6).

One can see that according to the minimum temperature reached during cooling, the DSC crystallization temperature shifts; the lower the cooling temperature, the lower the crystallization temperature. Below 425 °C, the crystallization temperature saturates at 600 °C.

The effect of cooling rate was also studied. In this case, samples were nucleated for 20 min at 500 °C and the temperature was decreased down to 400 °C, with two different cooling rates (10 or 30 °C/min), before running non-isothermal DSC experiments (Fig. 7). One can see that despite the cooling rate variation, the crystallization temperature was 600 °C.

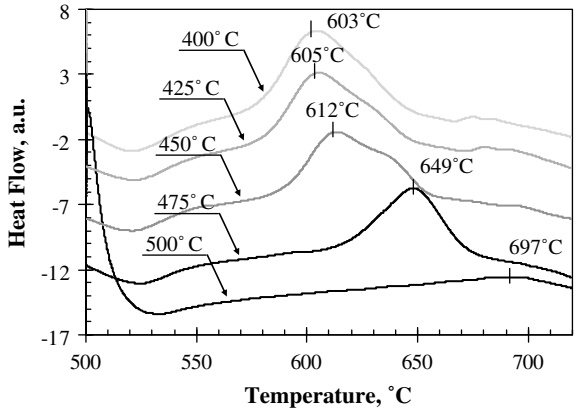

Fig. 6. DSC thermograms of UV-exposed PTR glass after 20 min pre-nucleation at 500 °C and 10 °C/min cooling down to a temperature between 400 and 500 °C.

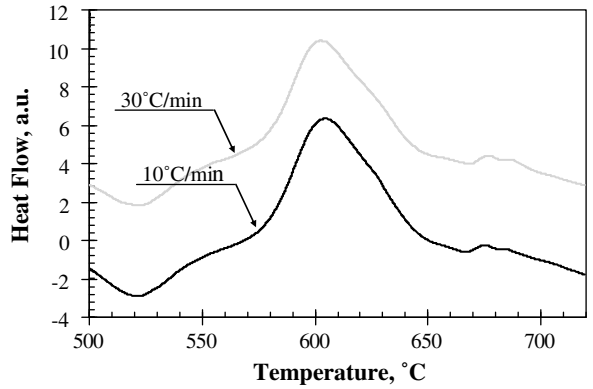

Fig. 7. DSC thermograms of UV-exposed PTR glass after 20 minutes pre-nucleation at 500 °C and 10 or 30 °C/min cooling down to 400 °C.

3.4. Effect of cooling on the absorption spectra of PTR glass

In order to gain more insight into the reactions that take place during cooling, we investigated the influence of cooling on the absorption spectra of UV-exposed PTR glass. The setup in Fig. 1 was used and the thermal treatment schedule is shown in Fig. 2c. The temperature was increased up to ~500 °C. Isothermal heat-treatment was carried out for about 20 min at 500 °C. At the end of this stage, transmitted power measurement ($P_{S1}(\lambda)$) was performed and the temperature was decreased down to ~400 °C with a rate of ~10 °C/min. After temperature stabilization, measurement of the transmitted power ($P_{S2}(\lambda)$) was performed at this lower temperature before increasing again up to 500 °C. After temperature stabilization, one last measurement of the transmitted power ($P_{S3}(\lambda)$) was performed. Fig. 8 illustrates the absorption spectra measured at each stage of the thermal treatment. One

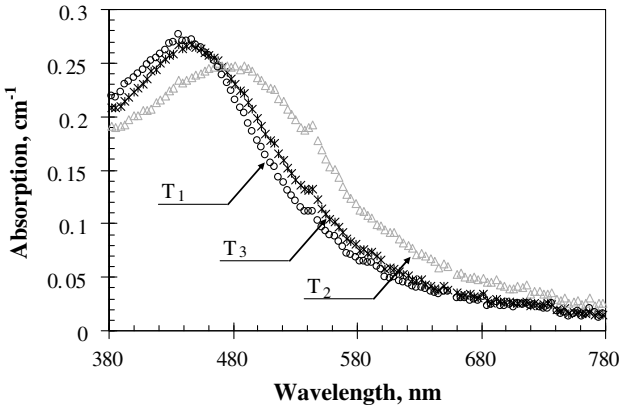

Fig. 8. Absorption band of silver containing particles measured at different stages of thermal treatment – black stars and circles show absorption spectra measured at 500 °C before and after cooling down to 400 °C, respectively and gray triangles show absorption spectra measured at 400 °C.

Table 1
Parameters of the Gaussian functions that were used for the decomposition of the absorption spectra of silver containing particles

Band	G_1	G_2	G_3	G_4
Central wavelength, nm	372	452	528	591
Bandwidth, cm^{-1}	4107	3363	2463	5671
Element	Hole	AgBr1	AgBr2	AgBr

can see that each spectrum is different depending on the sample temperature. The spectra measured at 500 °C are almost identical and have an overall absorption band centered at about 450 nm, whereas the spectrum measured at lower temperature has an overall absorption band centered at a larger wavelength, i.e. ~485 nm. As shown in Ref. [17], this overall absorption band is, in fact, a complex superposition of several Gaussian absorption bands (Table 1) that can be associated with different species. As a matter of fact, it has been shown in Ref. [18], that when PTR glass is exposed to short pulse radiations, it appears an absorption band around 360 nm which is typical of the glass matrix photoionization and that corresponds to the appearance of hole centers. When exposed to CW UV-radiation, this band only appears after thermal development, but is very similar to the one that was demonstrated in Ref. [18]. Therefore, the band with central wavelength at 360 nm was associated with hole centers. In order to understand the origin of the band centered at longer wavelengths, we melted glass without bromine [19]. Then, samples were ground and polished and were UV-exposed and thermally developed. Absorption spectra were measured, and then silver containing particles absorption was extracted and decomposed with Gaussian functions. It was shown that this decomposition can be performed with only two bands: one centered at 370 nm and one centered at 410 nm, and none of the bands having central wavelength above 410 nm was required [17,19]. Also, no band in the visible range appeared if no silver is added. These experiments thus demonstrated that both bromine and silver are contributing to these absorption bands, and it is therefore possible to associate the bands with central wavelengths at 452, 528 and 591 nm to some silver bromide containing particles. Also, it has been shown in Ref. [17], that these bands evolve in different ways during the thermal development. Hence, they are most likely associated with different types of silver bromide containing particles. We applied this method for the decomposition of each of the three absorption spectra.

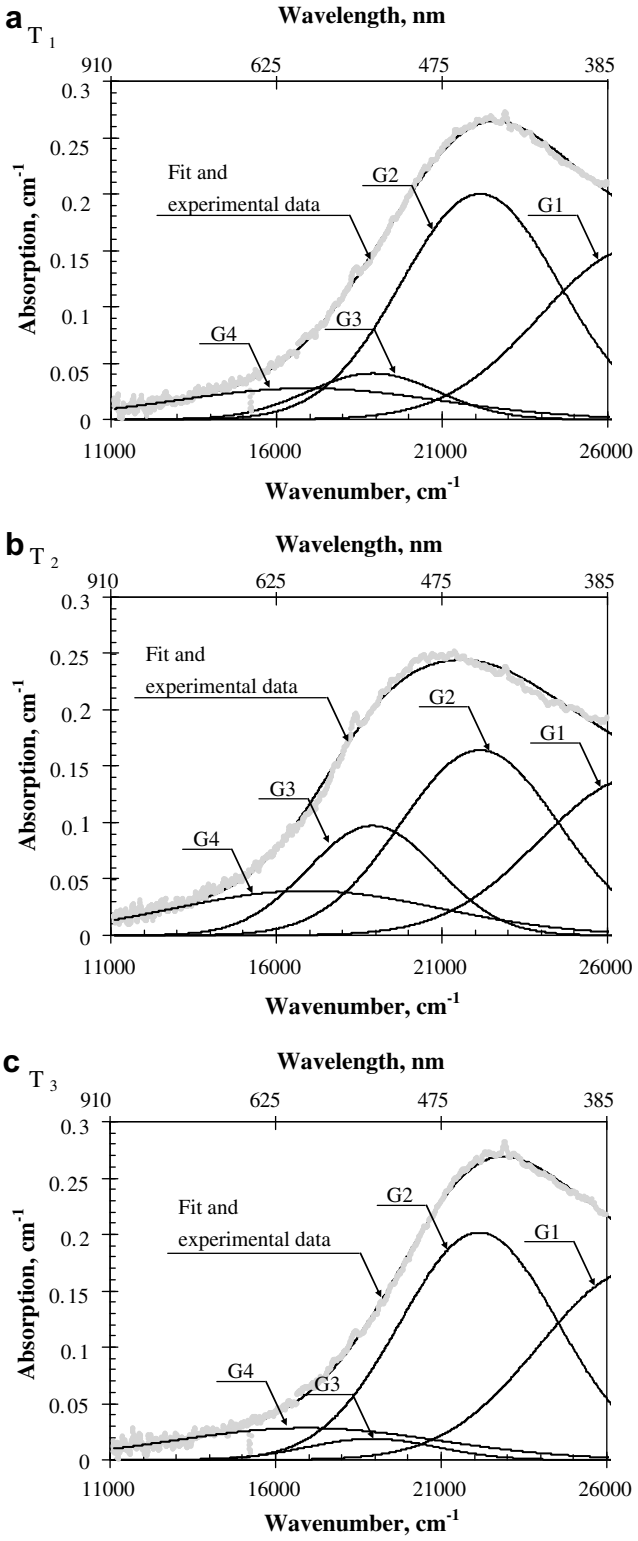

Fig. 9. Decomposition of the absorption spectra of silver containing particles using Gaussian functions – T_1: measurement carried out at 500 °C before cooling down to 400 °C, T_2: measurement carried out at 400 °C and T_3: measurement carried out at 500 °C after cooling down to 400 °C.

Table 2
Amplitude of the Gaussian functions used for fitting the absorption spectra of silver containing particles measured at T_1, T_2, and T_3

	T_1	T_2	T_3
G_1	0.15	0.14	0.17
G_2	0.20	0.16	0.20
G_3	0.04	0.10	0.02
G_4	0.02	0.04	0.02

Table 1 summarizes the bands that were used for this decomposition. Each band has a fixed position and spectral width and optimization was attained with minimization of the distance between the theoretical and experimental curves, while only separately changing the amplitude of each Gaussian band. Fig. 9 illustrates the fit of each absorption band and Table 2 the amplitude of each Gaussian band. One can see that the band at 370 nm is almost the same regardless the temperature, and the band at 530 nm is negligible at high temperatures, but appears at low temperatures; whereas the band at 450 nm decreased its amplitude by about 20%. In addition to these observations, we can conclude that the reactions that occur during cooling, and lead to the optical absorption variations mentioned above, appear to be reversible.

4. Discussion

Photo-thermo-refractive glass is photosensitive. UV-exposure followed by thermal treatments can lead to significant refractive index change. However, the mechanisms underpinning such refractive index change are not fully understood. It is well known that the glass has to be heat-treated at temperatures above T_g to exhibit a refractive index change in the UV-exposed regions. A correlation between refractive index change and thermal treatment temperature and/or duration was previously demonstrated [17]. However, up to now, no correlation was tested between the

cooling schedule and crystallization, and ultimately refractive index change. Fig. 3 shows the evolution of the refractive index change versus the minimum temperature reached before quenching after 30 min of heat-treatment at 520 °C. There is a quasi-linear relationship between the refractive index change measured at room temperature and at the minimum temperature reached before quenching. This result shows that not only the crystallization temperature is important to promote refractive index change, but also the cooling rate. It is worth noting that if further heat-treatments are performed, the effect of cooling becomes not as important as that of the first heat-treatment, i.e. refractive index change occurs even if a sample is quenched directly from the development temperature.

In order to have a better picture about the mechanisms that occur during cooling, we first investigated the influence of cooling on the PTR glass microstructure. Fig. 4 shows the microstructure of the UV-exposed PTR glass after six successive 5-min heat-treatments at 650 °C, and a single 30-min heat-treatment at 650 °C. One can see that crystals are larger after continuous 30-min thermal treatment than after six consecutive 5-min heat-treatments. Moreover, large dendrites appear after continuous heat-treatment, while only very small dendrite-like crystals can be seen after multi-stage heat-treatments. Fig. 5 illustrates quantitatively this result by showing growth of the largest crystals in each glass. Once more, it is obvious that the kinetics of crystallization in PTR glass do not only depend on the thermal development temperature and duration, but also on the cooling steps during heat-treatment. Moreover, it can be seen in Fig. 4 that the number of crystals is not very different whether single step or multi-step heat-treatment is used. One shall remember that these micrographs were taken with an optical microscope and, therefore, do not show crystals smaller than half micron diameter. Also, the fluorine content in PTR glass is ~2 mol%, which means that crystallization occurs in limited fluorine content and the crystal size saturates when all the fluorine has been consumed. In other words, this result indicates that the insertion of a cooling step in the heat-treatment schedule has an additional impact on the PTR glass crystallization.

Two mechanisms can be proposed to explain the effect of cooling. The first one is that cooling catalyzes the nucleation process and allows the appearance of a large number of crystals, which are smaller than the resolution of the optical microscope. Such crystals quickly consume the available fluorine and, therefore, prevent the growth of large crystals. The other mechanism is that cooling induces some type of liquid phase separation (fluorine rich areas), which hinders the diffusion of fluorine through the liquid droplets and, therefore, the growth of large crystals. The presence of small crystals or different glassy phases can be confirmed in Fig. 4. The second phase appears surrounding the large crystals, as a fine structure, which can be associated with the appearance of either small crystals or liquid phase separation. The effect of changing the cooling schedule can also be observed at macro-scale. Samples that underwent multi-step heat-treatments are very white and opaque, confirming the presence of a fine structure that induces significant scattering of the visible light. X-ray diffraction measurements carried out on these samples would permit to confirm whether this effect is due to some crystalline [6] or glassy phase.

Further study of the effect of cooling on crystallization of UV-exposed PTR glass was performed by non-isothermal DSC and in situ pre-nucleation. Fig. 6 shows the evolution of the DSC traces measured after 20 min nucleation at 500 °C followed by a temperature decrease down to a given temperature between 400 and 500 °C. It is seen that if temperature is decreased below 450 °C, the crystallization temperature measured by DSC reaches a minimum of ~600 °C. If the temperature is not decreased after the pre-nucleation step, crystallization temperature lies within the same range of temperatures than that for PTR glass UV-exposed but not pre-nucleated [20]. Finally, if the temperature is decreased to between 450 and 500 °C, the crystallization peak shifts to a temperature between 600 and 720 °C. In fact, it was demonstrated by Lumeau et al. [20] that the use of an adequate pair of nucleation temperature and duration allows reaching a minimum temperature in UV-exposed PTR glass equal to 600 °C. For example, it was shown that 20 min at 500 °C allows reaching this minimum temperature. In that reference, the study was carried out using two-stage heat-treatments. Pre-nucleation was performed in a calibrated furnace and samples were quenched from the nucleation temperature down to room temperature. Hence, in Lumeau et al.'s experiments, the temperature was decreased below 450 °C before being measured by DSC, and no attention was given to the importance of the cooling step after pre-nucleation. In this paper, we show that not only the nucleation temperature and duration are important to enhance nucleation, but also the cooling step below ~450 °C after pre-nucleation plays an important role. Finally even if the cooling rate has a role on the refractive index change measured after the first heat-treatment in PTR glass, Fig. 7 shows that the cooling rate causes no measurable impact on crystallization measured by DSC. Therefore these results show that only the minimum reached temperature is important, not the cooling rate. This conclusion is supported by the fact that a large shift in the crystallization temperature was observed in quenched samples in Ref. [20].

Up to this point, all the results shown in this paper were obtained by either an indirect method (DSC) or after freezing the process (refractive index change, optical micrographs) and, therefore, did not allow us to understand what is happening during the process itself. To perform such in situ study, we developed a high temperature spectroscopic setup (Fig. 1), and measured the absorption spectra of PTR glass at high temperatures (400 and 500 °C). In this way, we were able to reveal some of the mechanisms which occur during the cooling process. It was shown in Ref. [17] that the absorption band of silver containing particles, which is centered in the visible part of the spectrum between 400 and 500 nm, plays a key role in the nucleation process. It was also demonstrated that this band can be decomposed into elementary Gaussian bands and that a new band centered at 530 nm appears when PTR glass undergoes maximum nucleation (appearance of a reddish coloration). Fig. 8 shows the evolution of absorption spectra of UV-exposed PTR glass, in the process of nucleation. First of all, when PTR glass reached maximum nucleation (i.e. after 20 min at 500 °C), the overall silver containing particles absorption band is centered at about 450 nm. Then, as soon as the temperature is decreased down to 400 °C, this band appears to shift to longer wavelengths, ~485 nm. Decomposition into Gaussian functions (Fig. 9) shows that there is no shift of any band, but a change of the structure of this overall-band. As shown in Table 2, the main absorption band at 500 °C is that of silver bromide – centered at about 450 nm –- and the band at 530 nm is almost negligible (within the experimental error). But, when the temperature is decreased down to 400 °C, about 20% of the band at 450 nm is bleached out and converted into a new band at 530 nm. Analysis of the absorption spectrum measured after new heating at 500 °C shows that iterative heating to 500 °C results in total destruction of the 485-nm overall-band and restoration of 450-nm overall-band.

These observations are relevant since they show that this band at 530 nm appears only at low temperatures and is associated with the maximum of the nucleation in PTR glass. Moreover, particles that make this overall-band appear are most likely associated to silver bromide. As the melting point of (macroscopic) silver bromide is 428 °C [21], the need to decrease the temperature below 450 °C can be explained by the fact that silver bromide is expected

to be liquid when a sample is kept at 500 °C; and the phase that has an absorption band at 530 nm only appears when these particles solidify. This supposes that the absorption band at 530 nm can be ascribed to nucleation centers which control photo-induced crystallization and induce the observed refractive index decrement. With these results, we can infer that photo-induced crystallization is efficient only if such nucleation centers, with absorption band centered at 530 nm, appear, and if the temperature is decreased below 450 °C. Otherwise, only spontaneous crystallization will occur and this fact explains why the microstructure and crystallization kinetics observed without cooling are very similar to those of samples that were neither UV-exposed nor pre-nucleated.

5. Conclusion

The effects of cooling rate and final cooling temperature on UV-exposed PTR glass were examined. We demonstrated that it is necessary to decrease the temperature after the pre-nucleation treatment in order to observe the typical refractive index decrement of PTR glass. We first showed that the main part of the refractive index change observed after a single stage heat-treatment in PTR glass takes place during the cooling step from 520 °C down to 420 °C, and then saturates.

Identical behavior was observed on the microstructure of UV-exposed PTR glass. We have shown that the use of multi-step heat-treatment (including some cooling steps) induces smaller crystals and a finer structure, which was associated with the appearance of liquid phase separation or very tiny crystals.

The effect of cooling on nucleation was also analyzed. We demonstrated that the decrease of temperature down to 400 °C after the nucleation process is necessary to obtain a significant shift of the DSC crystallization peak. This result is an indirect proof that cooling is a mandatory step in order to benefit from the pre-nucleation treatment.

Finally, the evolution of the spectro-photometric properties of PTR glass during cooling was monitored. We showed that cooling of UV-exposed PTR allows the creation of a new phase with absorption band at 530 nm. We ascribed this band to nucleation centers which control photo-induced crystallization and induce the refractive index decrement.

Acknowledgements

This work was partially supported by DARPA contracts HR-01-1041-0004 and HR-0011-06-1-0010. JL acknowledges the IMI-NFG support (NSF Grant No. DMR-0409588). EDZ and GPS acknowledge funding by CNPq (Brazil). EDZ also thanks FAPESP (contract # 2007/08179-9).

References

[1] S.D. Stookey, Ind. Eng. Chem. 41 (1949) 856.
[2] V.A. Borgman, L.B. Glebov, N.V. Nikonorov, G.T. Petrovskii, V.V. Savvin, A.D. Tsvetkov, Sov. Phys. Dokl. 34 (1989) 1011.
[3] O.M. Efimov, L.B. Glebov, L.N. Glebova, K.C. Richardson, V.I. Smirnov, Appl. Opt. 38 (1999) 619.
[4] O.M. Efimov, L.B. Glebov, S. Papernov, A.W. Schmid, Proc. SPIE 3578 (1999) 554.
[5] O.M. Efimov, L.B. Glebov, V.I. Smirnov, Opt. Lett. 23 (2000) 1693.
[6] T. Cardinal, O.M. Efimov, H.G. Francois-Saint-Cyr, L.B. Glebov, L.N. Glebova, V.I. Smirnov, J. Non-Cryst. Solids 325 (2003) 275.
[7] L.B. Glebov, V.I. Smirnov, C.M. Stickley, I.V. Ciapurin, in: W.E. Tompson, P.H. Merritt (Eds.), Laser Weapons Technology III, Proceedings of SPIE, Vol. 4724, 2002, p. 101.
[8] O. Andrusyak, V. Rotar, A. Sevian, V. Smirnov, G. Venus, L. Glebov, in: 20th Annual Solid State and Diode Laser Technology Review, SSDLTR-2007 Technical Digest, BC2-2, Los Angeles, CA, June 2007.
[9] D. Stookey, G.H. Beall, J.E. Pierson, J. Appl. Phys. 49 (1978) 5114.
[10] O.M. Efimov, L.B. Glebov, H.P. Andre, Appl. Opt. 41 (2002) 1864.
[11] L.B. Glebov, L. Glebova, Glass Sci. Technol. 75 (C2) (2002) 294.
[12] Leonid Glebov, Larissa Glebova, Victor Tsechomskii, Valerii Golubkov, in: Proceedings of XX International Congress on Glass, Kyoto, Japan, September 2004, O-07-082.
[13] Marvin Hass, James W. Davisson, Herbert B. Rosenstock, Julius Babiskin, Appl. Opt. 14 (5) (1975) 1128.
[14] J. Lumeau, L. Glebova, L.B. Glebov, J. Non-Cryst. Solids 354 (2008) 425.
[15] L.B. Glebov, Glass Sci. Technol. 75 (C1) (2002) 73.
[16] J. Lumeau, A. Sinitskiy, L.N. Glebova, L.B. Glebov, E.D. Zanotto, Optical and crystallization homogeneity of photo-thermo-refractive glass, Glass and Optical material division, Spring 2006 Meeting (Greenville, South Carolina, USA), Paper GOMD-S3-007-2006, May 2006.
[17] J. Lumeau, L. Glebova, L.B. Glebov, in: Proceeding of the International Congress on Glass paper M3, 2007.
[18] Leo Siiman, Julien Lumeau, Leonid B. Glebov, Nonlinear photosensitivity of photo-thermo-refractive glass by high intensity laser irradiation, J. Non-Cryst. Solids, in press, doi: 10.1016/j.jnoncrysol.2008.05.051 .
[19] L. Glebova, J. Lumeau, M. Klimov, E.D. Zanotto, L.B. Glebov, J. Non-Cryst. Solids 354 (2008) 456.
[20] J. Lumeau, A. Sinitskiy, L.N. Glebova, L.B. Glebov, E.D. Zanotto, Phys. Chem. Glasses: Eur. J. Glass Sci. Technol. B 48 (4) (2007) 281.
[21] V.M. Nield, D.A. Keen, W. Hayes, R.L. McGreevy, J. Phys: Condens. Matter 4 (1992) 6703.